Fokker-Planck Modeling for AT Applications[†]

Advanced Tokamak Workshop, General Atomics, March 9-11, 1999

Outline of Talk

- Situations in which kinetic Fokker-Planck modeling is needed
- Equations solved by the CQL3D bounce-averaged FP code.
- Examples BAFP modeling applied to
  - LHCD in Asdex
  - ECH in DIII-D
  - FW+NBI
- Radial transport of nonthermal distributions
- Bootstrap calculation for nonthermal distributions
- Plans
- Concluding remarks

[†]R.W. Harvey, CompX, Del Mar, CA.

Situations Where Fokker-Planck Modeling is Indicated

- Due to variation of the Coulomb collision frequency ($\propto v^{-3}$), nonthermal features are generally observed in the tails of the electron or ion distibutions.
- RF electron CD efficiency is proportional to v_{phase}^2/n_e for $v_{phase} > v_{Te}$

  $\Longrightarrow$ Pushes experiments towards high phase velocity, low density

  $\Longrightarrow$ For ECCD, substantial tail formation occurs if $p_{EC}(W/cm^3) > 0.5(n_{13}^2/(v_{phase}/2v_{Te})^2$.
  Nonthermal effect on CD for $n_{13} <$ 3-4,
  tail diagnostic effects to larger density.

  $\Longrightarrow$ For LH, tail formation is a ubiquitous feature of high power experiments.
- Pellet injection leads to large induced toroidal electric fields providing prompt runaways and knock on avalanche.
- LH enhanced knock-on runaway production may be a feature in LHCD experiments (V.S. Chan, 1999).
- Radial transport leads to nonthermal tail, when $\tau_{slowing} > \tau_{transport}$. This was observed on ALC-A. Its possible effects on global transport depend on the velocity dependence of the transport coefficients. In any case, a radial diffusion operator in a FP code provides a natural way to treat the coupling between particle, momentum and energy transport.
- Bootstrap current can be enhanced by elevated tail distributions (due to RF and NBI) and modified by RF scattering (LH).
- There are important nonthermal effects in edge divertor plasma which are properly treated by Fokker-Planck codes but will not be covered here.

GENERAL ATOMICS

CQL3D: 3D Bounce-Averaged Fokker-Planck Code for ECH/LH/FW/NBI

Solves the coupled equations:

$$(1)\ \frac{\partial}{\partial t}(\lambda f) = \frac{\partial}{\partial \underline{u}_0} \cdot \left[\underline{\Gamma}_{DC} + \underline{\Gamma}_{RF} + \underline{\Gamma}_{coll} \right] + R(f) + S_{NB}$$

- $\underline{\Gamma}_{DC}$: DC ELECTRIC FIELD
- $\underline{\Gamma}_{RF}$: RF QL OPERATOR
- $\underline{\Gamma}_{coll}$: NL COLLISIONS (FP)
- $R(f)$: RADIAL DIFFUSION AND CONVECTION
- S_{NB}: NB DEPOSITION

(2) RF energy equation, along rays:

$$\nabla \cdot \left(\underline{v}_{group}\, \mathcal{E} \right) = -P_{absorbed} = -\int \underline{du}\, (\gamma - 1)\, mc^2\, Q(f)$$

$Q(f)$: QL OPERATOR

(3) NBI Source (FREYA)

(4) Equilibrium Equation

$$\nabla^* \Psi = \mu_0 J_\phi$$

CQL3D Assumptions

- Diffusive processes (Fokker-Planck)
- Coulomb collisions
- Quasilinear RF
- Neglect RF particle pinch
- Azimuthally symmetric distributions about B_{mag} in velocity ($\tau_{cyclotron} << \tau_{coll}$)
- Bounce average ($\tau_{bounce} < \tau_{coll}$)
- Zero banana width
- Toroidal geometry
- Up-down symmetric noncircular equilibria

GENERAL ATOMICS

Numerical Approach to B_0

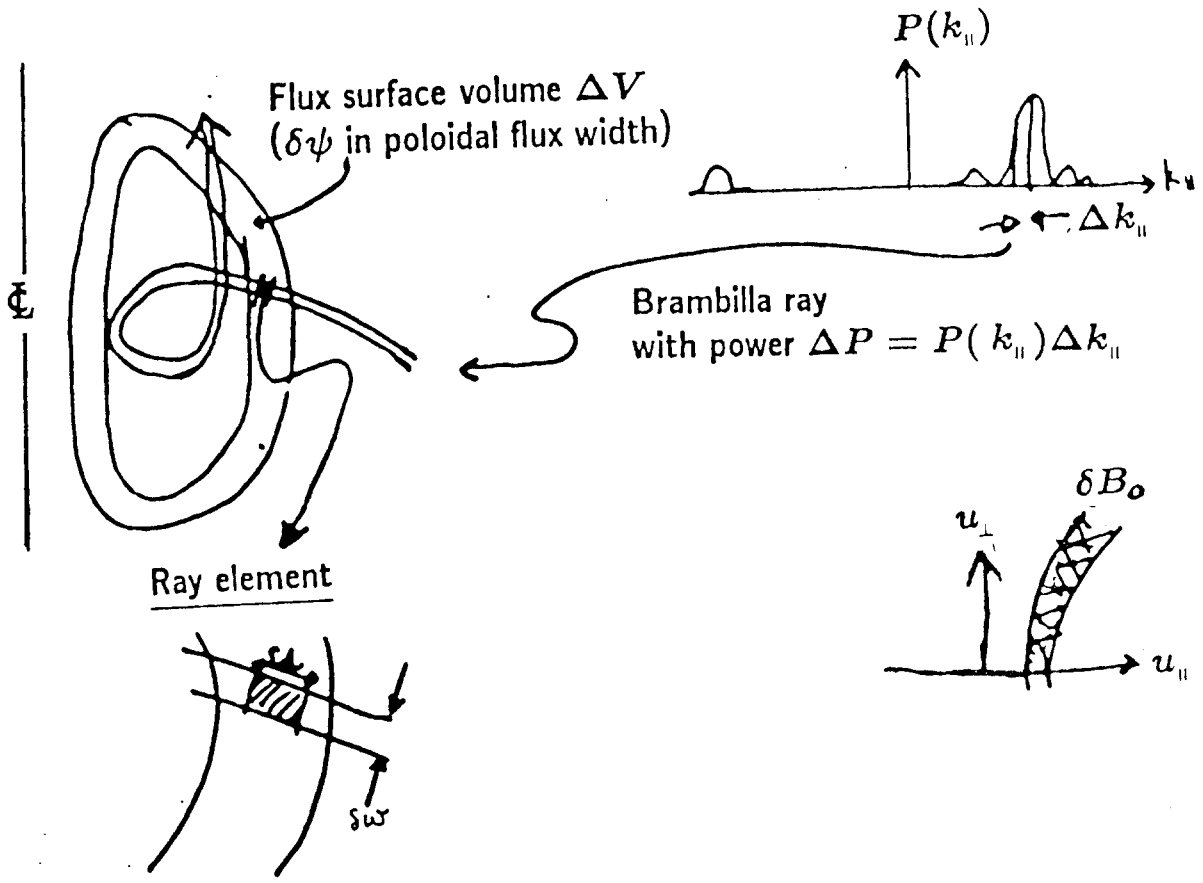

$$\delta B_0 = \frac{1}{\Delta V} \int dV \oint \frac{d\ell_B}{|u_{\parallel}|} u^2 \cos^2\theta \, D_{\parallel}$$

↑ Local QL diffusion coefficient

$$D_{\parallel} = \frac{\pi e^2}{2 m_e^2} \left(\frac{n_{\parallel} u}{\gamma c}\right)^2 \frac{\gamma}{|u_{\parallel}|} \left| u_{\parallel} J_0\left(\frac{k_{\perp} u_{\perp}}{\omega_{ce}}\right) E_z + i u_{\perp} J_1\left(\frac{k_{\perp} u_{\perp}}{\omega_{ce}}\right) E_y \right|^2$$

$$P_{abs} = \int d^3v \, (\gamma - 1) \, mc^2 \left.\frac{\partial f}{\partial t}\right|_{QL}$$

GENERAL ATOMICS

CQL3D Radial Diffusion and Convection Operator

$$R(f) \sim \frac{1}{\rho}\frac{\partial}{\partial \rho}\left(D_{\rm pp}\frac{\partial f}{\partial \rho} + V_{\rm p} f\right) \qquad \text{(circular)}$$

$$\equiv \frac{u_{\parallel 0}}{B_{\rm min}} \frac{\int (d\ell_B/\psi)}{H\rho} \left.\frac{\partial}{\partial \rho}\right|_{C_1,C_2} H\rho \frac{B_{\rm min}}{u_{\parallel 0}} \qquad \text{(noncircular)}$$

(conservative form)

$$\times \left\{ D_{\rho\rho} \left.\frac{\partial}{\partial \rho}\right|_{C_1,C_2} \left[\frac{\lambda}{\int (d\ell_B/\psi)} f\right] + \frac{V_\rho \lambda f}{\int (d\ell_B/\psi)} \right\}$$

where

ℓ_B = Distance along $\underline{B}$-field line on a flux surface

ψ = $B/B_{\rm min}$ ($B_{\rm min}$ = minimum B along ℓ_B)

H = ONETWO (Hinton & Haseltine) Volume Factor

= $(dV/d\rho)$ / $(4\pi^2 R_0 \rho)$

C_1, C_2 = Velocity Space constants of radial diffusion:

Presently: ① v_0, θ_0

<u>or</u> ② E, μ

*The 3 D equations are solved by a fully implicit velocity radial-splitting scheme (a method originally explored by Greg Hammett).

GENERAL ATOMICS

CQL3D is Coupled to Major Codes in the Community

- RAYLH — Brambilla Ray Tracing Code for LH and Fast Waves
- TORCH — LLNL EC Ray Tracing
- FREYA — NBI Deposition (ORNL)
- SELENE — 2D Noncircular Equilibria (JAERI)
- HORACE — Electron Cyclotron Emission Diagnostic (GA-Culham)
- XRAY — Xray Bremsstrahlung Diagnostic

GENERAL ATOMICS

Asdex Combined 90° and 180° Spectra Give Current Profile Control

(Two independent "grills": 750 kW from 90°-phased grill, overlapped with additional 300 kW from 180°-phased grill)

$n_{e0} = 2 \times 10^{13}$/cc, $T_{e0} = 4.5$ keV

Central ($r = 0.1\,a$) QL diffusion coefficient versus $u_\parallel$, $u_\perp$:

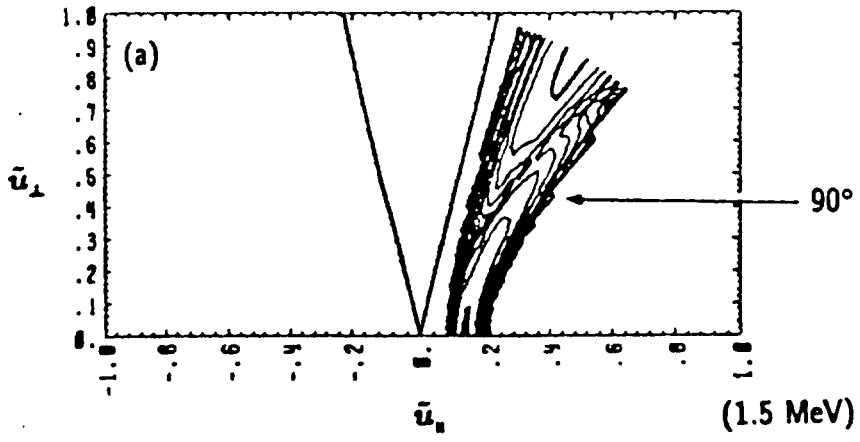

$r = 0.54\,a$ — QL diffusion coefficient versus $u_\parallel$, $u_\perp$:

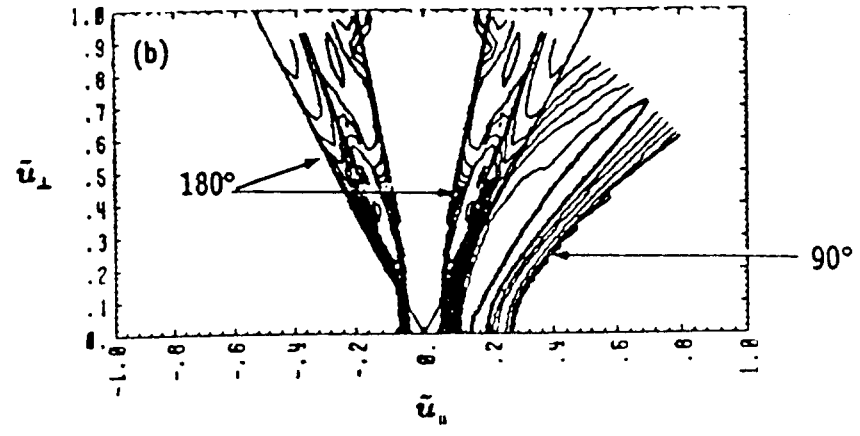

GENERAL ATOMICS

Electron Distribution Function $f(u_{\parallel}, u_{\perp})$ at $\rho = 0.5\,a$

Contour of f versus $u_{\parallel}$ and $u_{\perp}$:

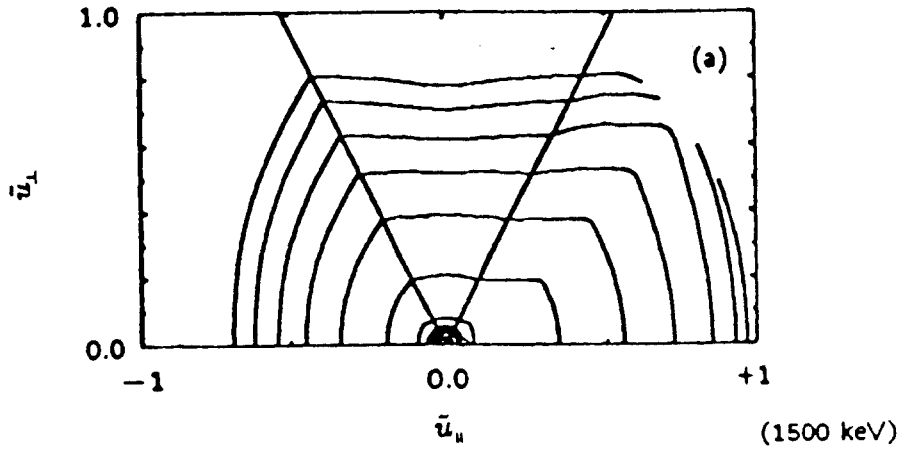

Slices through f at constant pitch angle:

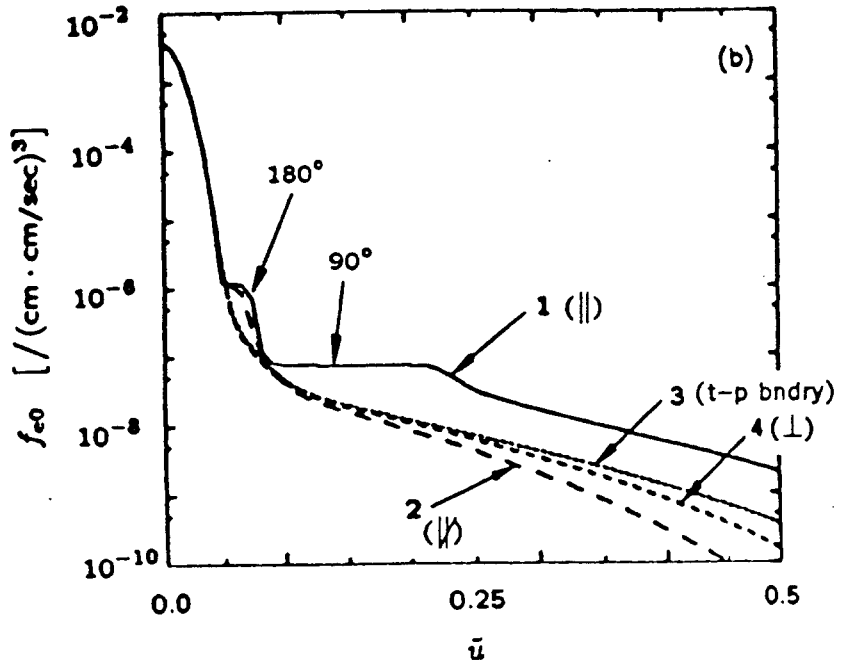

GENERAL ATOMICS

Calculated Power Deposition and Driven Current

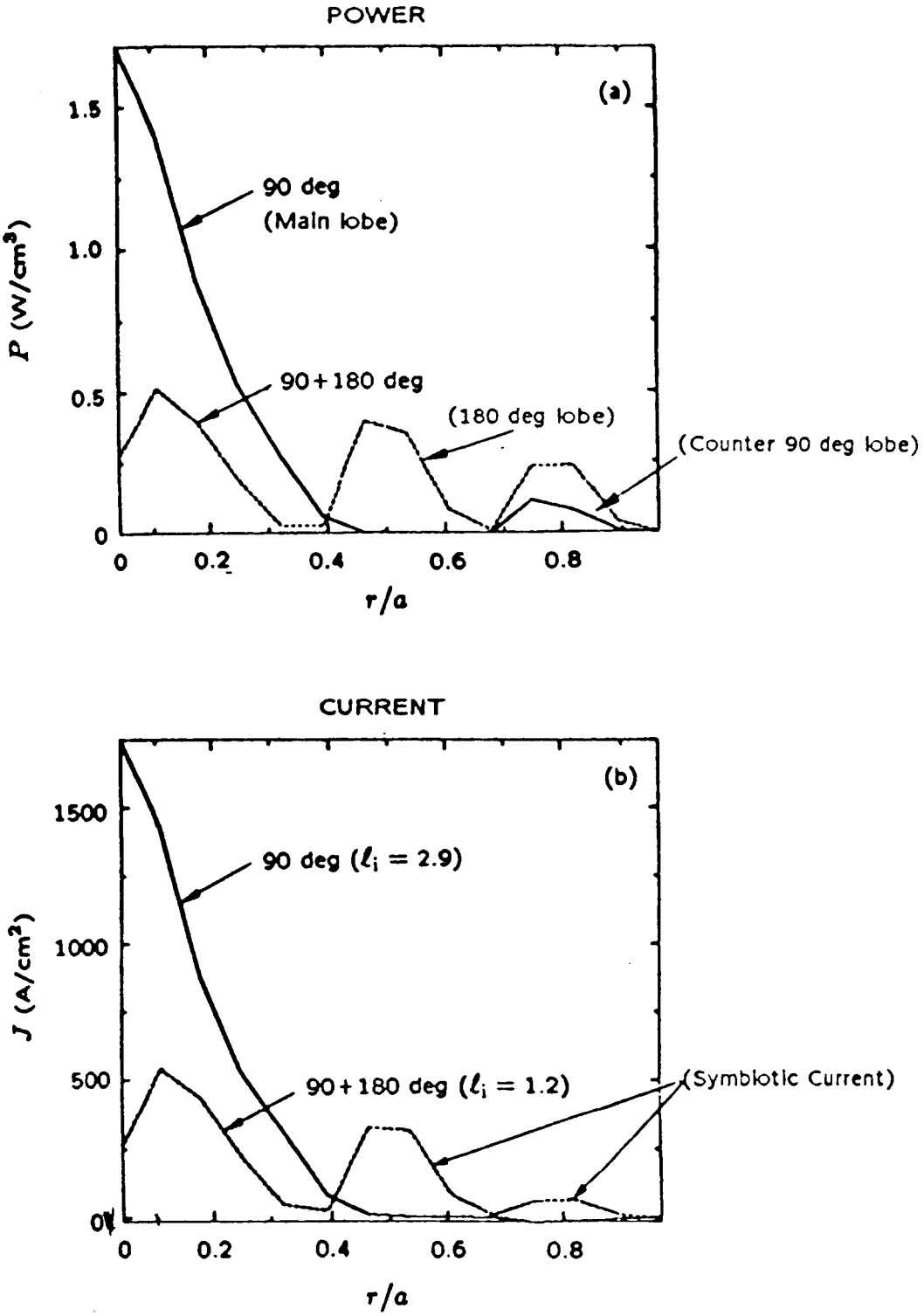

GENERAL ATOMICS

Conclusions on CQL3D/LH Modeling of ASDEX

1. Current drive efficiency agrees with experiment.

2. Agreement with anisotropy and ℓ_i changes from ohmic (except too peaked in central current drive cases), over a range of 90°, $-90°$, $90° + 180°$, 180°, and 120° phasing cases.

3. The code provides a quite reliable means to estimate current profile control.

4. Demonstrates the physics of spectral gap filling and efficient current profile control by mixed spectra.

EXPERIMENTAL DEPENDENCE OF E_{dc} IS MODELED WELL BY CQL3D

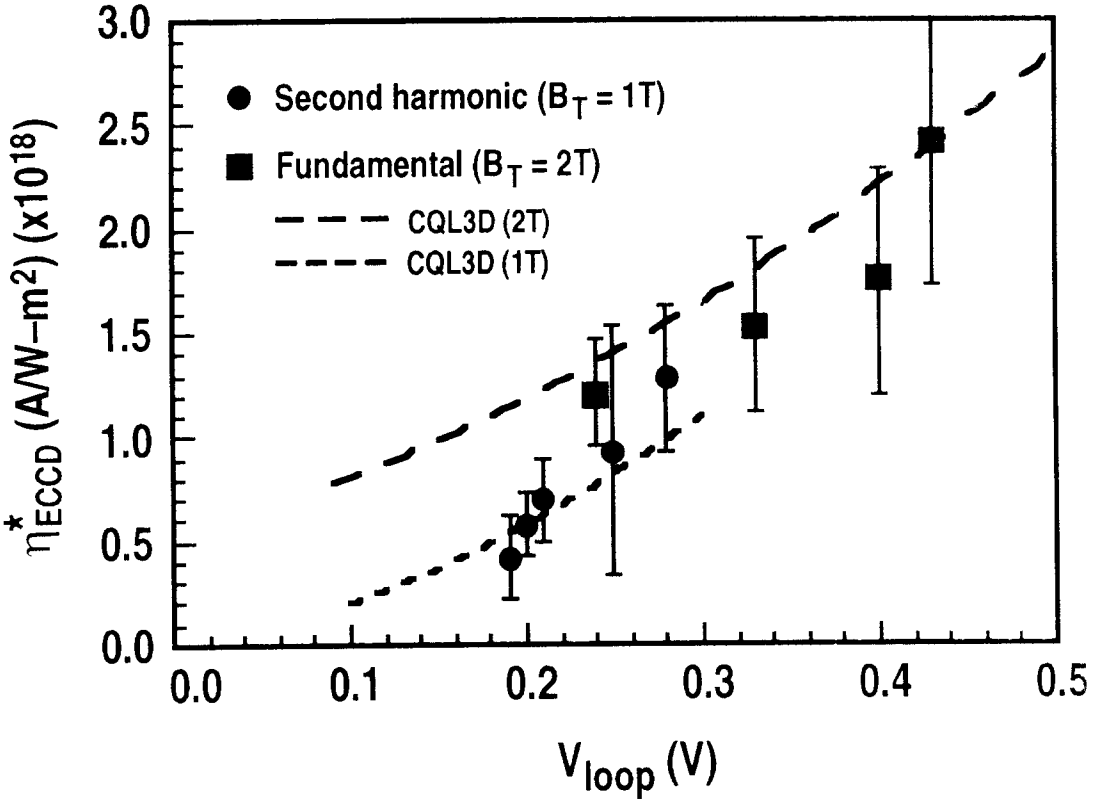

- $\eta^* = \dfrac{n_e I_{rf} R_m}{P_{rf}}$ with finite E_{dc}
- $E_{dc} = V_{loop}/2\pi R_m$

R.A. James, et al., "Electron Cyclotron Current Drive Experiments in the DIII–D Tokamak," Phys. Rev. A 45, 8783 (1992).

C.C. Petty, et al., "Fast Wave and Electron Cyclotron Current Drive in the DIII–D Tokamak," accepted for publication in Nucl. Fusion

GENERAL ATOMICS

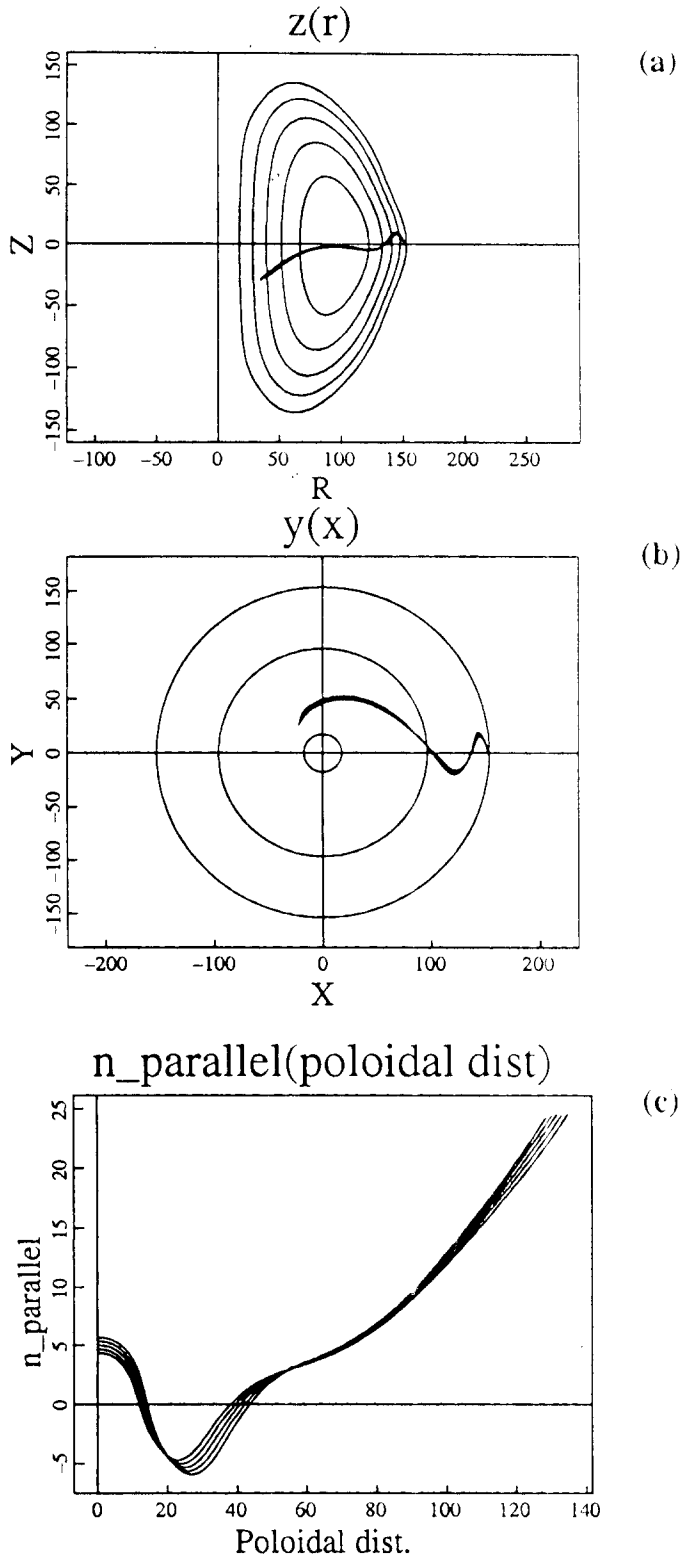

Fig. 1. (a) Poloidal view of 30 MHz HHFW rays, n_par=3-4, propagating into 5% beta NSTX equilibrium. n(0)=1.e14 cm**3, T(0)=1 keV plasma, parabolic profiles. (b) Top view of rays. (c) Variation of parallel refractive index along the ray. The magnetic axis occurs at about 65 cms. poloidal distance.

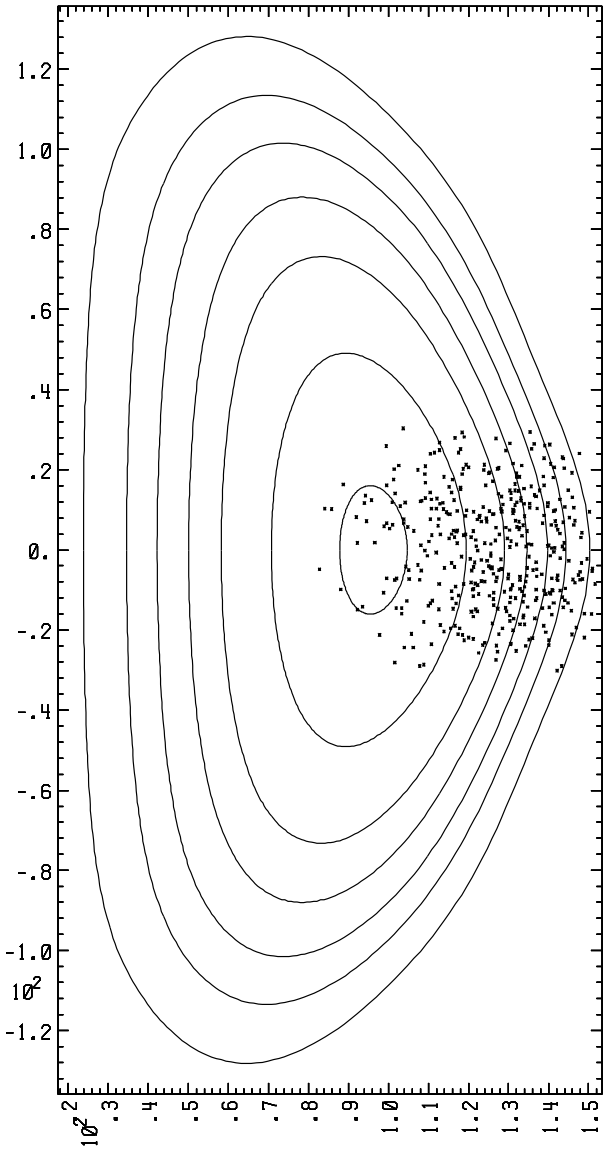

Fig. 2. Birth points for fast ions calculated with the FREYA neutral beam deposition code. Beam injection energy is 80 keV, with 70% H+, 20 % H2+, and 10 % H3+ ions from the source. The plasma has n(0)=1.e14/cm**3, T(0)=1 keV.

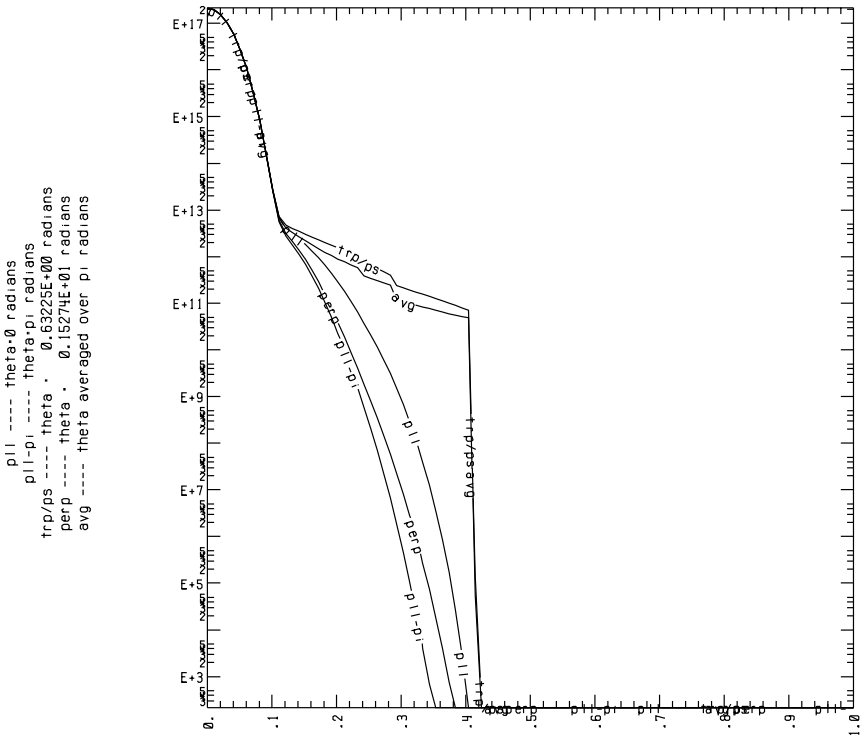

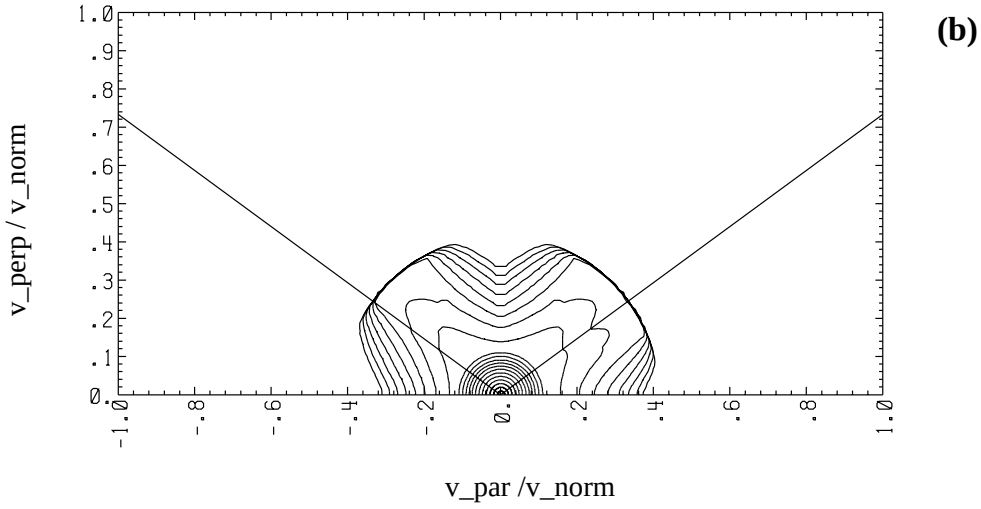

Fig. 3. Hydrogen ion distribution function at plasma radius r/a=0.6 Maximum energy on the grid is 500 keV, giving the velocity normalization v_norm. (a) Cuts of the ion distribution versus velocity, at constant pitch angles as indicated. (b) Contour plot of the distribution, versus v_parallel and v_perpendicular. This is for a case of 80 keV neutral beam injection only.

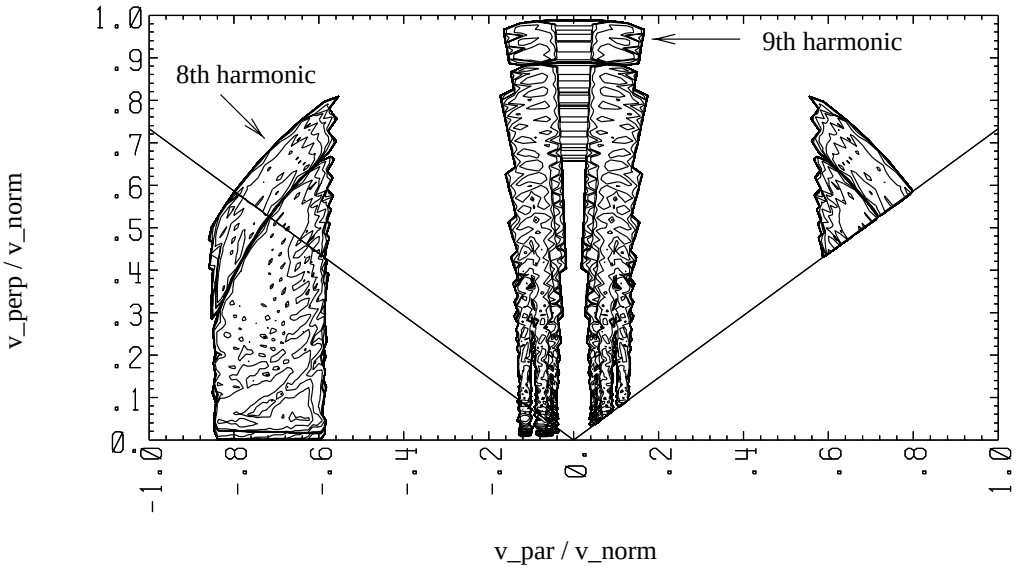

Fig. 4. Contour plot of the v**2*D_vv quasilinear diffusion coefficient in v_parallel, v_perp -space. This is at r/a=0.6. Maximum velocity on the grid is as in Fig. 3. Only five HHFW rays, shown in Fig. 1, have been used to form the diffusion coefficients, hence the graininess of the coefficient. At this plasma radius, the 9th harmonic hydrogen ion absorption is dominant.

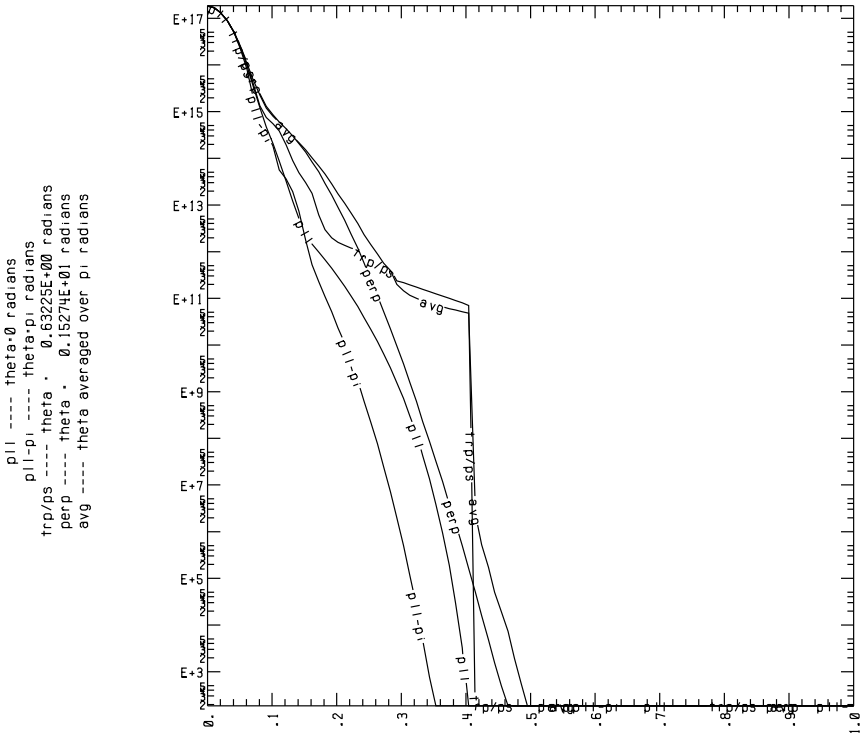

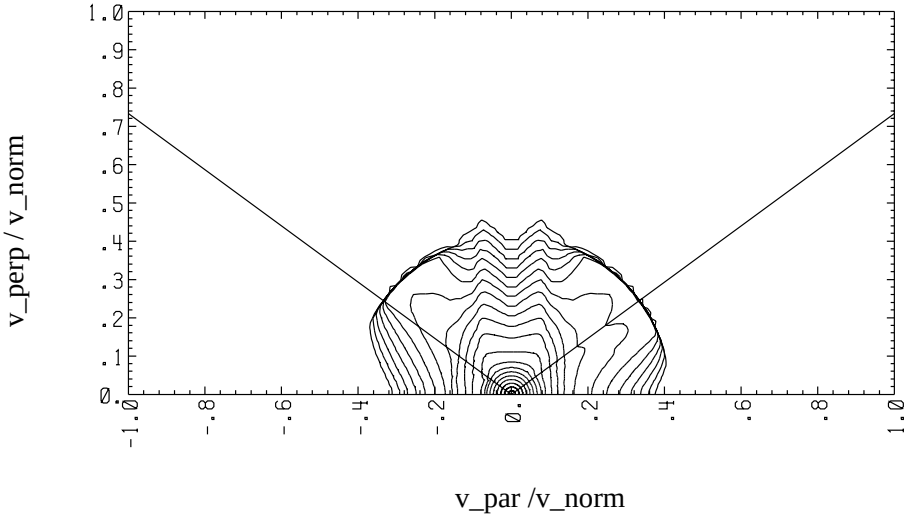

Fig. 5. Hydrogen ion distribution function at plasma radius r/a=0.6, resulting from a combination of HHFW and neutral beam injection. Parameters are as in Fig. 3. (a) Cuts of the ion distribution versus velocity, at constant pitch angles, as indicated. (b) Contour plot of the distribution, versus v_parallel and v_perpendicular. The HHFW has inflated the distribution in the perpendicular velocity direction.

Enhanced/Modified Bootstrap Current

- Bootstrap current is enhanced by
  1. elevated electron and/or ion tail distributions
  2. added RF pitch angle diffusion
- These effects can be seen from the parallel momentum balance equation:
  For $j_{banana} = -ev_{\|}\rho_{L,poloidal}\ \partial n_{trap}/\partial\rho$,
  we have $(j_{bootstrap}/en)\nu_{ei} = (\nu_{\perp}/\epsilon)m_e(j_{banana}/en)$,
  where $\nu_{ei} \propto v^{-3}$,
  $and(\nu_{\perp}/\epsilon)$ is the effective collision frequency for detrapping.
- CQL3D calculates the enhanced bootstrap current by introducing a jump into the velocity space boundary conditions at the trapped-passing boundary, of size $\rho_{L,poloidal}\partial f_{e,i}/\partial\rho$ [Harvey *et al.*, Sherwood Theory 1993; Westerhof and Peters, CPC, 1995].

  This model gives "good" agreement with the Hinton and Haseltine expression for banana regime bootstrap current.
- The model has been applied to DIII-D ECCD experiments to explain enhanced ECCD as reported by Luce [IAEA, 1998], but for this case the collisions were dominating the pitch angle collisions.
- A substantial effect has been shown in connection with LHCD, and needs further follow up work.

COMPARISON OF NUMERICALLY CALCULATED BOOTSTRAP CURRENT WITH RESULTS OF HINTON & HASELTINE (Rev. of Modern Physics)

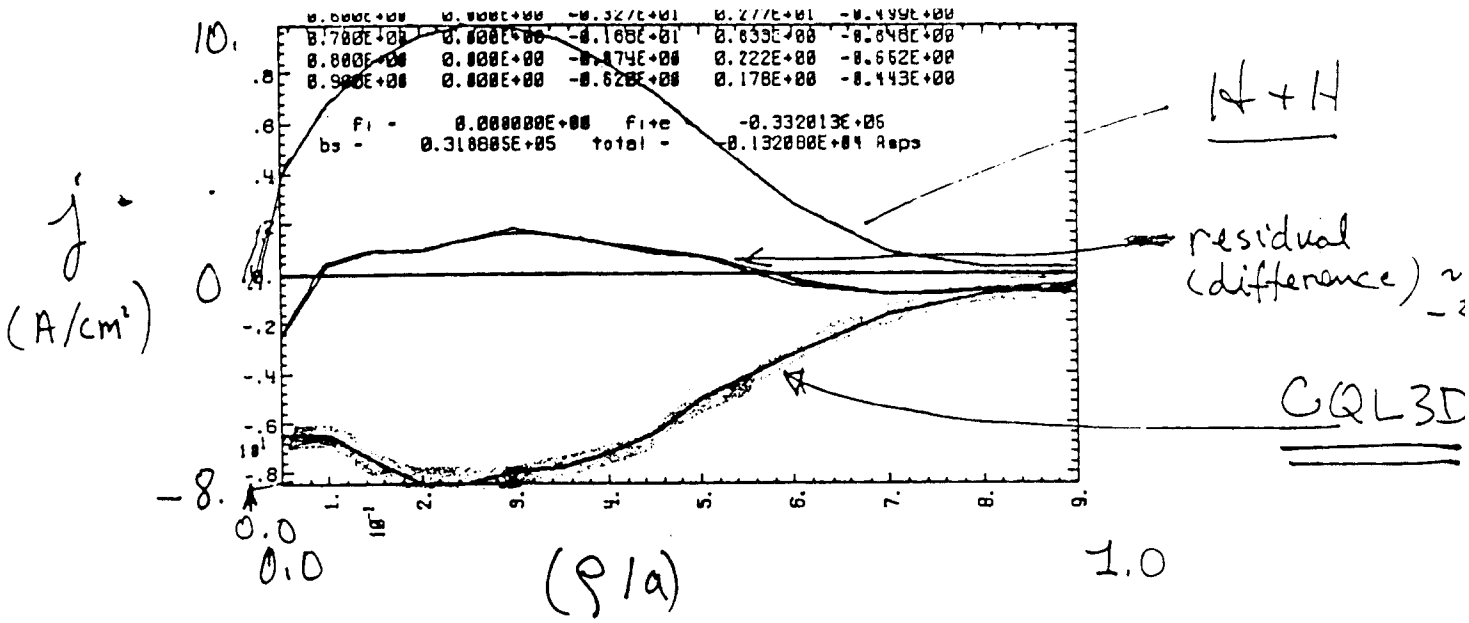

BOOTSTRAP CURRENT:

CQL3D → 33.2 kA

H+H → 31.9 kA

3% OVERALL

DIFFERENCES: 1) COURSENESS OF CQL3D RADIAL MESH.

2) CQL3D IS A FINITE AS

LOWER HYBRID EDGE CURRENT DRIVE IN VH MODE.

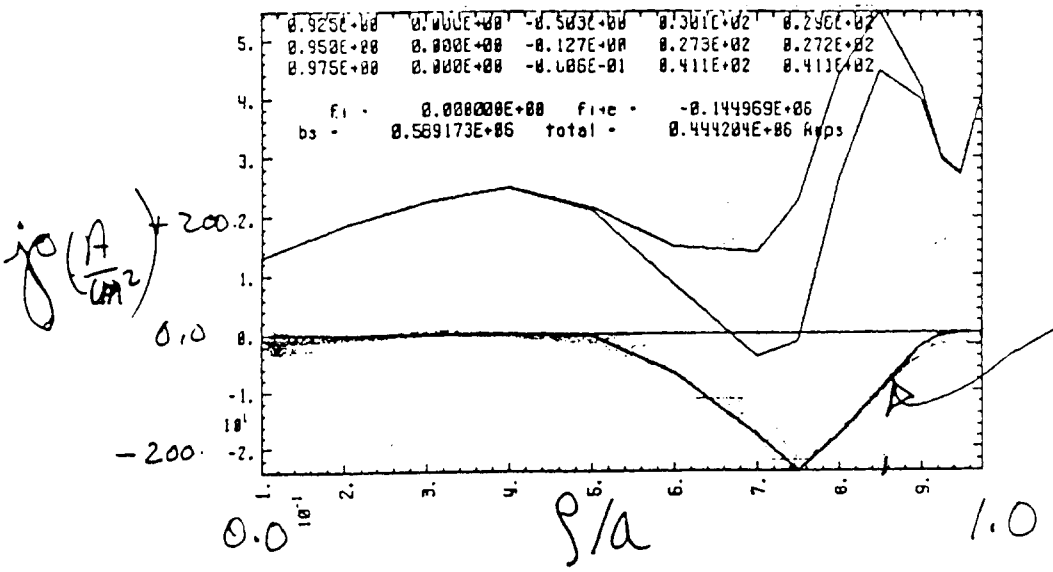

RF CURRENT
(LHCD)
CQL3D
-145 kA.

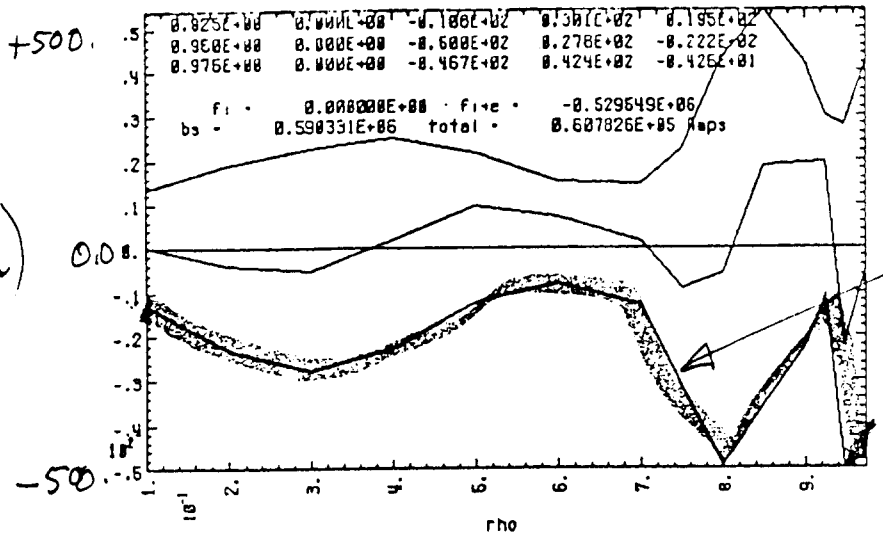

$j_{bootstrap}$
(No LH)
CQL3D
-530 kA

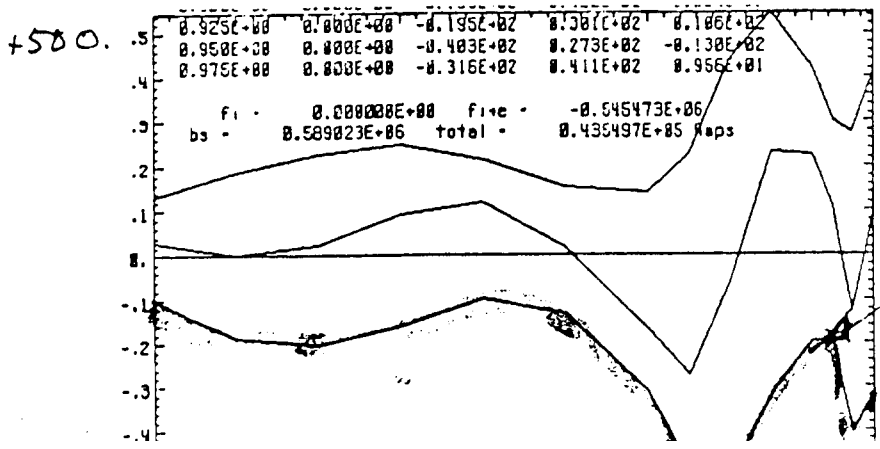

$j_{LHCD} + j_{bootstr}$
CQL3D
-545.5 kA

EFFECT OF TRANSPORT ON ELECTRON TAIL, INDICATED BY LOSS RATE OFF G

NO TRANSPORT

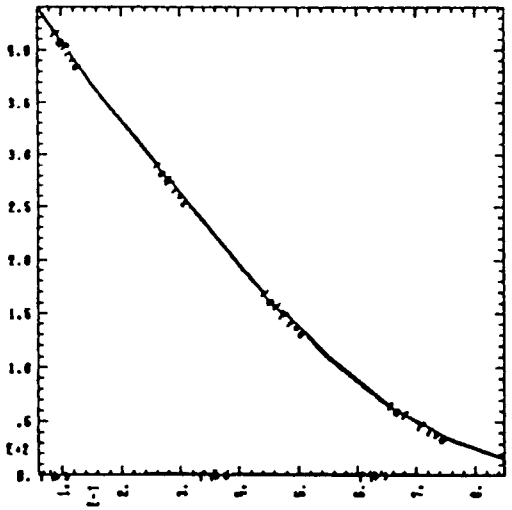

RUNAWAY "PROFILE"

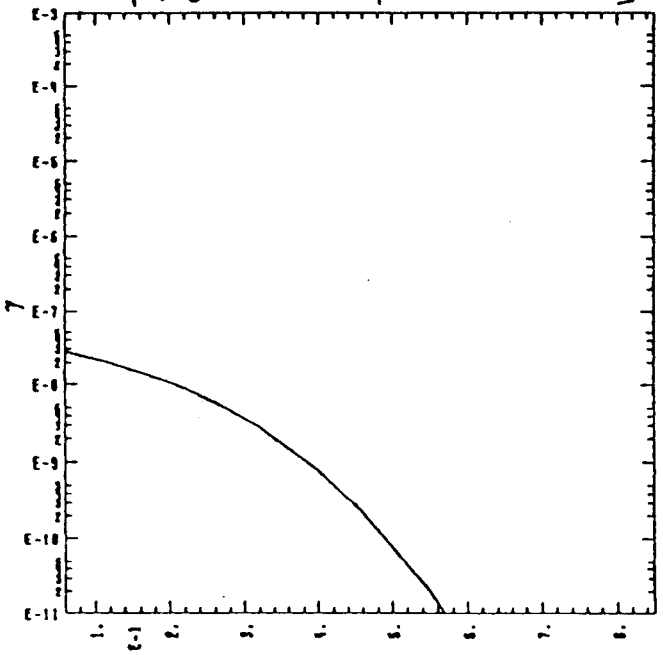

WITH TRANSPORT

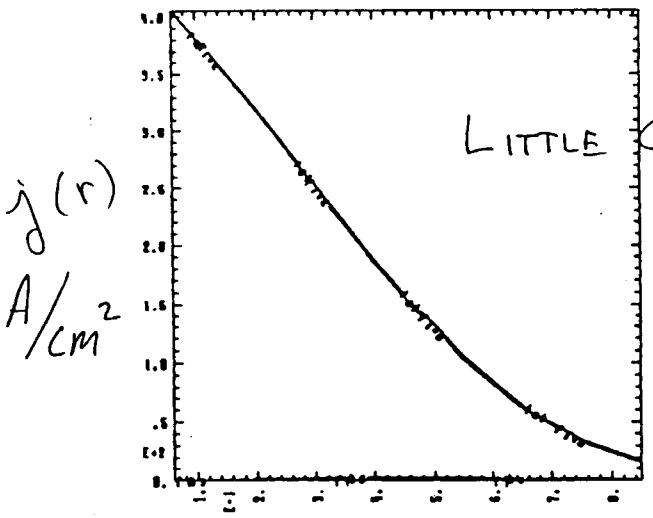

LITTLE CHANGE.

RUNAWAY "PROFILE"

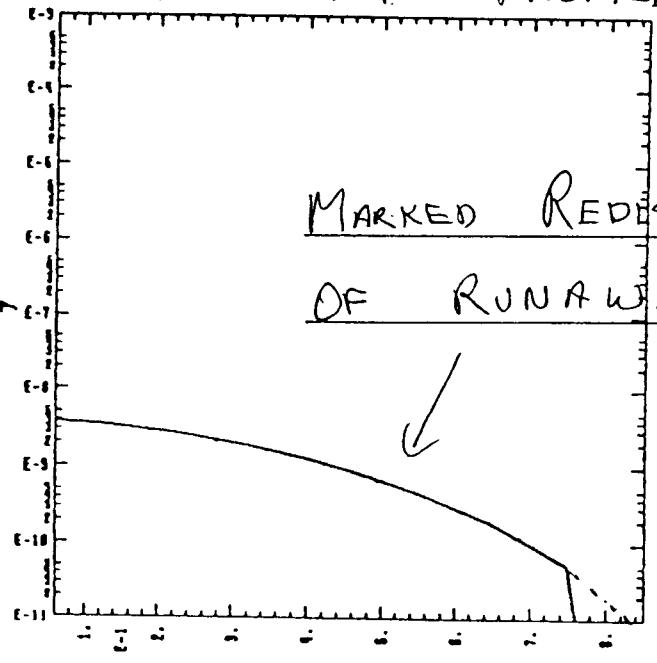

MARKED REDISTRIBUTION OF RUNAWAYS

Code Development Plans

- **Add Ampere-Faraday Maxwell equations to obtain the self-consistent toroidal electric field as a function of radius and time.**
- **Add ripple and banana losses.**

Concluding Comments

- **The Fokker-Planck approach in CQL3D has a broad range of useful applications, particularly for high power current drive situations in experimental AT plasmas.**